Biogeosciences, 17, 3083–3097, 2020
https://doi.org/10.5194/bg-17-3083-2020

Biogeosciences Open Access EGU

A revised pan-Arctic permafrost soil Hg pool based on Western Siberian peat Hg and carbon observations

Artem G. Lim[1], Martin Jiskra[2], Jeroen E. Sonke[3], Sergey V. Loiko[1], Natalia Kosykh[4], and Oleg S. Pokrovsky[3,5]

[1]BIO-GEO-CLIM Laboratory, Tomsk State University, Tomsk, Russia
[2]University of Basel, Environmental Geosciences, Bernoullistrasse 30, 4056 Basel, Switzerland
[3]Geosciences and Environment Toulouse, UMR 5563 CNRS, 14 Avenue Edouard Belin, 31400 Toulouse, France
[4]Lab Biogeocenol, Institute of Soil Science and Agrochemistry, Russian Academy of Sciences, Siberian Branch, Novosibirsk, Russia
[5]N. Laverov Federal Center for Integrated Arctic Research, Russian Academy of Sciences, Arkhangelsk, Russia

Correspondence: Oleg S. Pokrovsky (oleg.pokrovsky@get.omp.eu)

Received: 8 December 2019 – Discussion started: 28 January 2020
Revised: 29 April 2020 – Accepted: 19 May 2020 – Published: 18 June 2020

Abstract. Natural and anthropogenic mercury (Hg) emissions are sequestered in terrestrial soils over short, annual to long, millennial timescales before Hg mobilization and run-off impact wetland and coastal ocean ecosystems. Recent studies have used Hg-to-carbon (C) ratios (R_{HgC}'s) measured in Alaskan permafrost mineral and peat soils together with a northern circumpolar permafrost soil carbon inventory to estimate that these soils contain large amounts of Hg (between 184 and 755 Gg) in the upper 1 m. However, measurements of R_{HgC} on Siberian permafrost peatlands are largely missing, leaving the size of the estimated northern soil Hg budget and its fate under Arctic warming scenarios uncertain. Here we present Hg and carbon data for six peat cores down to mineral horizons at 1.5–4 m depth, across a 1700 km latitudinal (56 to 67° N) permafrost gradient in the Western Siberian Lowland (WSL). Mercury concentrations increase from south to north in all soil horizons, reflecting a higher stability of sequestered Hg with respect to re-emission. The R_{HgC} in the WSL peat horizons decreases with depth, from 0.38 Gg Pg^{-1} in the active layer to 0.23 Gg Pg^{-1} in continuously frozen peat of the WSL. We estimate the Hg pool (0–1 m) in the permafrost-affected part of the WSL peatlands to be 9.3 ± 2.7 Gg. We review and estimate pan-Arctic organic and mineral soil R_{HgC} to be 0.19 and 0.63 Gg Pg^{-1}, respectively, and use a soil carbon budget to revise the pan-Arctic permafrost soil Hg pool to be 72 Gg (39–91 Gg; interquartile range, IQR) in the upper 30 cm, 240 Gg (110–336 Gg) in the upper 1 m, and 597 Gg (384–750 Gg) in the upper 3 m. Using the same R_{HgC} approach, we revise the upper 30 cm of the global soil Hg pool to contain 1086 Gg of Hg (852–1265 Gg, IQR), of which 7 % (72 Gg) resides in northern permafrost soils. Additional soil and river studies in eastern and northern Siberia are needed to lower the uncertainty on these estimates and assess the timing of Hg release to the atmosphere and rivers.

1 Introduction

High-latitude organic-rich soils are key ecosystems controlling the transfer of carbon, nutrients, and pollutants between the atmosphere, rivers, lakes, and the Arctic Ocean. These soils are most vulnerable to ongoing climate change due to the high-potential mobility of carbon stored in the form of peat deposits. Part of the peat layers is currently frozen but may be subjected to fast thawing, especially in discontinuous- and sporadic-permafrost zones (Romanovsky et al., 2010). While the stock of C in Arctic and sub-Arctic peat and mineral soils is fairly well quantified (472 Pg C; 95 % confidence interval, CI, of ±27 Pg) in the upper 0–1 m (Hugelius et al., 2014), this is not true for pollutants such as mercury (Hg). Because of its strong bioamplification in Arctic marine biota (Morel et al., 1998) and exposure to native Arctic populations (AMAP, 2011), there is a strong interest in understanding Hg biogeochemistry in Arctic environments (Outridge et al., 2008; Steffen et al., 2008; Stern et al., 2012).

Recent advances in quantifying Arctic Hg cycling show that Arctic Hg^{II} wet deposition is generally low (Pearson et al., 2019) and that the vegetation Hg pump drives year-long net gaseous Hg^0 (and CO_2) deposition via foliar uptake to Arctic vegetation and litterfall to soils (Obrist et al., 2017; Jiskra et al., 2018, 2019). Soil core analyses in Alaska indicate that large amounts of carbon and Hg have accumulated since the last glacial maximum (Olson et al., 2018; Schuster et al., 2018). Two upscaling approaches reported differing estimates for the 0 to 1 m soil pool of the northern circumpolar permafrost region of 184 Gg (Olson et al., 2018) and 755 Gg (Schuster et al., 2018).

Despite the overall net atmospheric Hg deposition to soils, research has found that Arctic rivers export 37 to 44 $Mg\,yr^{-1}$ of soil Hg, bound to particulate and dissolved organic matter, to the Arctic Ocean (Fisher et al., 2012; Dastoor et al., 2014; Zhang et al., 2015; Sonke et al., 2018; Zolkos et al., 2020). Together with coastal erosion of soils (30 $Mg\,yr^{-1}$), river Hg inputs constitute a terrestrial Hg flux of 74 $Mg\,yr^{-1}$ to the Arctic Ocean that is of similar magnitude to gross atmospheric deposition (80 $Mg\,yr^{-1}$) over the Arctic Ocean (Sonke et al., 2018). Permafrost thawing has been shown to enhance river Hg export from soils to rivers (St. Pierre et al., 2019). It is most pronounced in the discontinuous-permafrost zone due to thawing of fresh soil organic matter and maximal active layer depth and has been suggested to potentially double over the next 50 years (Lim et al., 2019). The quantity of atmospheric Hg deposition to northern peat soils that is presently re-emitted to the atmosphere is not well understood. Hg exchange studies indicate temporally limited Hg^0 emission from the Alaskan permafrost tundra at 68° N (Obrist et al., 2017) and year-round net Hg^0 emission from Scandinavian peat at 64° N (Osterwalder et al., 2018). Other studies provide evidence for vegetation type (Rydberg et al., 2010) and temperature and insolation control (Fahnestock et al., 2019) on net Hg^0 deposition or emission.

All available data of Hg in permafrost soils originate from North America or Scandinavia (Jensen et al., 1991; Bailey et al., 2002; Talbot et al., 2017; Schuster et al., 2018; Olson et al., 2018). Except for in three studies (Golovatskaya et al., 2009; Lyapina et al., 2009; Vasilevich, 2018), we did not find extensive measurements of Hg in peat profiles from boreal and permafrost regions of the Russian Arctic and Siberia. Recent work has used a soil carbon model to estimate the size of the northern permafrost soil Hg inventory to be 755 ± 427 Gg (95 % CI) in the upper 1 m (Schuster et al., 2018). However, this estimate is based on extrapolation of high Hg-to-organic-carbon (C) ratios (R_{HgC}'s) of 1.6 Gg Hg per petagram of C ($Gg\,Pg^{-1}$) in Alaskan mineral soils to the entire North American and Eurasian permafrost zone. Another study used lower R_{HgC}'s of 0.12 to 0.62 $Gg\,Pg^{-1}$ derived from observations of both Alaskan organic and mineral soils and literature data, to estimate a lower northern soil 0–1 m Hg inventory of 184 Gg (136–274 Gg, 37.5–62.5 percentiles; Olson et al., 2018). Both studies provide the Hg inventory by multiplying the respective R_{HgC} by the same C pool estimates for the northern circumpolar permafrost region, covering an area of 17.8×10^6 km^2 (Hugelius et al., 2014).

Direct measurements of soil Hg and carbon profiles in frozen peatlands of Siberia are needed to address these variable R_{HgC} and Hg pool estimates of pan-Arctic permafrost soils. This constitutes the first and main objective of the present study. The second objective was to assess the impact of permafrost type (absent, sporadic, discontinuous, and continuous) on Hg concentrations and pools in the active layer, frozen peat, and mineral horizons. The third objective was to relate Hg concentration in peat to that of other trace metals in order to reveal possible mechanisms of Hg and other metal pollutant accumulation within the organic and mineral horizons of frozen peatlands. Finally, we revisit the world soil Hg inventory in order to put the pan-Arctic permafrost soil Hg pool into a global perspective.

2 Study site and methods

2.1 Sampling sites

Soil sampling was performed along a latitudinal transect of the Western Siberia Lowland (WSL) that comprised the southern taiga (Plotnikovo, 56° N), the middle taiga (Mukhrino, 60° N), the northern part of the taiga zone (Kogalym, 62° N), forest tundra (Khanymey, 62° N; and Pangody, 65° N), and tundra (Tazovsky, 67° N) biomes (Fig. 1). In the WSL, the permafrost zones follow the temperature and vegetation distribution over the latitude at otherwise similar relief, lithology, and runoff, thus allowing us to test the effect of permafrost by analyzing latitudinal features of Hg distribution in soils. Key physicogeographical parameters of studied sites and soil types are listed in Table S1 in the Supplement. The WSL peat actively formed since the beginning of the Holocene until freezing of bogs in the Subboreal period (11–4.5 kyr; Kremenetski et al., 2003; Panova et al., 2010; Ponomareva et al., 2012; Loiko et al., 2019). For 4.5 kyr, the rate of peat formation and bog extension in the permafrost-affected part of the WSL has been decreasing. In the southern part of the cryolithozone and permafrost-free part of the WSL, peat accumulation and bog extension remained active over the entire Holocene (Kurina and Veretennikova, 2015; Preis and Karpenko, 2015; Kurina et al., 2018). The main mineral substrates underlying frozen peat layers of the WSL are quaternary clays, sands, and alevrolites. In the southern part (Plotnikovo and Mukhrino sites), the typical substrate is carbonate-bearing clays of lake alluvium origin with rare layers of sandstones (Table S1).

Mean annual ambient temperature (MAAT) decreases from south to north, being equal to −0.4, −1.2, −4.0, −5.6, −6.4, and −9.1 °C at Plotnikovo, Mukhrino, Kogalym, Khanymey, Pandogy, and Tazovsky, respectively (Trofimova and Balybina, 2014). The permafrost is absent in Plot-

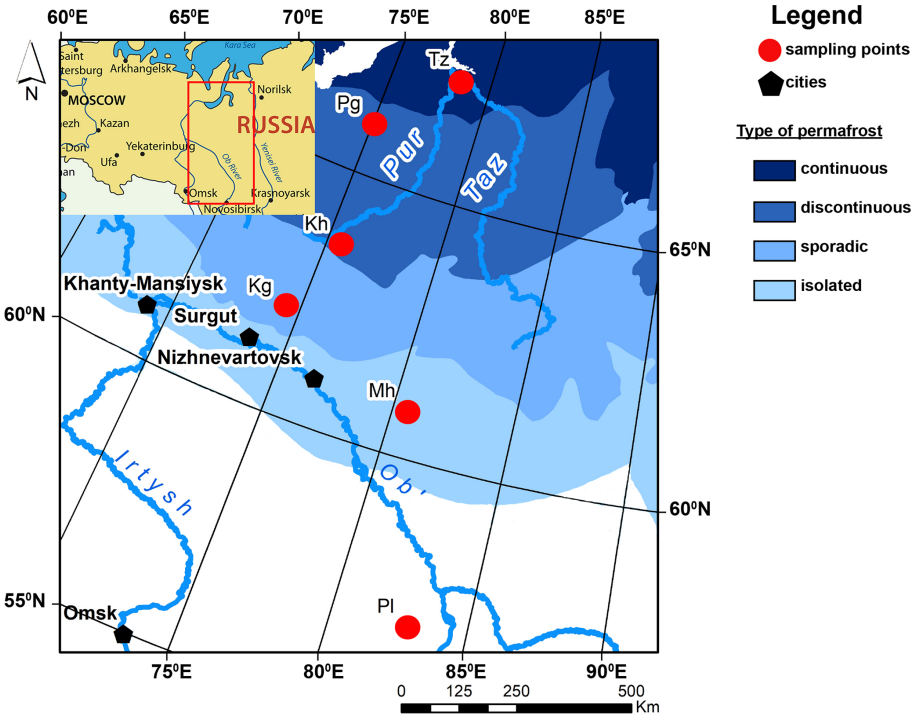

Figure 1. Sampling sites and permafrost boundaries (modified after Brown et al., 2001) of WSL territory investigated in this work. The climate and soil parameters of six sampling sites – Tazovsky (Tz), Pangody (Pg), Khanymey (Kh), Kogalym (Kg), Mukhrino (Mh), and Plotnikovo (Pl) – are listed in Supplement Table S1.

nikovo but present at all other sites, and it ranges from relict to isolated (Mukhrino) and isolated to sporadic (Kogalym) in the south to discontinuous (Khanymey, Pangody) and continuous (Tazovsky) in the north. At permafrost-affected sites, the average active-layer thickness (ALT) at the time of sampling of peat mounds (hummocks) ranged from 90 cm in the south to 45 cm in the north. The peat mounds of ombrotrophic bogs probed in this work are present across the full latitudinal gradient.

The vegetation of three studied types of bogs (polygonal, flat-mound, and ridge-hollow) is essentially oligotrophic (poor in nutrients) which indicates the ombrotrophic (rain- and snow-water-fed) conditions, i.e., the lack of groundwater input and lateral surface influx of nutrients. The flat-mound palsa is covered by dwarf shrubs (*Ledum decumbens*, *Betula nana, Andromeda polifolia, Vaccinium ssp., Empetrum nigrum*), lichens (*Cladonia ssp., Cetraria, Ochrolechia*), and mosses (*Dicranum ssp., Polytrichum ssp., Sphagnum angustifolium, S. lenense*). At southern sites, the pine *Pinus sylvestris* is abundant on ridges (Peregon et al., 2008, 2009), whereas the two taiga sites are dominated by *Pinus sylvestris*, with minor but permanently present *Betula pubescens* and *Pinus sibirica*. Dwarf shrubs are dominated by *Ledum palustre, Chamaedaphne calyculata*, and *Vaccinium vitis-idaea.* The moss layer is dominated by *S. fuscum*, *S. angustifolium*, with the presence of *S. magellanicum, S. capillifolium*, and boreal forest moss species like *Pleurozium schreberi*.

2.2 Sampling procedure, analyses, and data treatment

Peat core samples were collected in August, when the depth of the unfrozen layer was at its maximum (see Raudina et al., 2017). Based on measurements by temperature loggers over the summer period, the in situ temperature of the studied soil profile ranged from $15 \pm 5\,^{\circ}C$ in the top soil (0–20 cm) to $4 \pm 2\,^{\circ}C$ at the permafrost boundary (40–80 cm). Field logistics and financial resources did not make it possible to study multiple cores from each climate zone. The physical, chemical, and botanical properties of several peat cores collected in the homogeneous palsa region in the north and ridge–ryam complex in the south are highly similar among different peat mounds, suggesting that the cores we obtained are representative for the WSL (Velichko et al., 2011; Stepanova et al., 2015).

Peat cores were extracted using a Russian sediment–peat corer, and the frozen part was sampled using a motorized Russian peat corer (UKB-12/25 I, Russia) with a 4 cm diameter corer sterilized with 40 % ethanol prior to each extraction. We collected the full active (unfrozen) layer of the peat column, the frozen peat column and some 10 to 30 cm of frozen mineral horizons using clean powder-free vinyl gloves. Peat or mineral soil samples were divided in 5–10 cm segments using a sharp sterile single-use plastic knife. Soil samples were placed in sterile, doubled-zipped PVC bags and kept at $-20\,^{\circ}C$ during transport and storage. To avoid contami-

nation of peat from external surroundings, we separated the part of the core for geochemical analysis exclusively from the interior of the core (> 1 cm from the core liner) following conventional procedures (Wilhelm et al., 2011).

Total Hg concentration (THg) in freeze-dried and ground slices of peat cores was determined using a direct mercury analyzer (DMA-80, Milestone, Italy). Analysis of reference material BCR-482 (lichen, $480 \pm 28\,\mathrm{ng\,g^{-1}}$), MESS-3 (sediment, $91 \pm 9\,\mathrm{ng\,g^{-1}}$), and NIST SRM 1632d (coal, $93 \pm 3\,\mathrm{ng\,g^{-1}}$) showed good reproducibility (mean $\pm 1\sigma$) of 467 ± 28, 80 ± 6 and $98 \pm 8\,\mathrm{ng\,g^{-1}}$, respectively. The average uncertainty of duplicate sample analysis did not exceed 5 % (1σ). The carbon (C) and nitrogen (N) concentrations were measured using catalytic combustion, with Cu–O at 900 °C and an uncertainty of ≤ 0.5 %, using a Thermo Flash 2000 CN analyzer, aspartic acid (C 36.1 % ± 1.5 %; N 10.5 % ± 0.5 %), and soil reference material (C 2.29 % ± 0.07 %; N 0.21 % ± 0.01 %) as standards. Analyses of total C before and after sample treatment with HCl did not yield more than 1 % of inorganic C; therefore our total C determination represents organic carbon. For trace- and major-element analysis, soil samples were subjected to full acid digestion in the clean room following ICP-MS (inductively coupled plasma mass spectrometry; Agilent 7500 ce) analyses as described previously (Morgalev et al., 2017).

The Shapiro Wilk normality test was used to assess THg, elemental and R_{HgC} distributions, and statistical data descriptors adjusted accordingly. All statistical tests used a significance level of 95 % ($\alpha = 0.05$). Spearman rank order correlations (significant at $p < 0.05$) were performed to characterize the link of Hg with C, N, and other major and trace elements. The differences in Hg concentration between the active and frozen peat layer were tested using the Mann–Whitney U test for paired data at a significance level of 0.05.

C pools of different soil classes reported by Hugelius et al. (2014) were divided into two categories: organic and mineral soils. Histosols and Histels were defined as organic soils. Turbels and Orthels were considered as organic soils for the 0–0.3 m interval and as mineral soils for the 0.3–3 m interval. All other soils were considered as mineral soils. To estimate the pan-Arctic permafrost soil Hg pool, C pools were multiplied by the respective R_{HgC} derived for organic (> 20 % C) and mineral (< 20 % C) soil data from Eurasia and North America (excluding Alaska). To calculate the global Hg pool, a simpler approach was used, and one single R_{HgC} was considered for five climate zones, which were defined by latitude (Arctic: > 67° N; boreal: 50–67° N; temperate: 35–50° N; subtropical: 23.45–35° N; tropical: < 23.45° N) according to FAO and ITPS (2018). The uncertainty was assessed with a Monte Carlo approach using the *rnorm* and *rlnorm* functions of R (version 3.6.1.) and is reported as the interquartile range (IQR; 25th and 75th percentile) of 100 000 simulations. For the pan-Arctic permafrost soil Hg pool, final uncertainties incorporate the uncertainties of the C stock from Hugelius et al. (2014) assuming normal distribution and the uncertainties of R_{HgC} assuming log-normal distribution.

3 Results

3.1 Depth (vertical) distribution of Hg in WSL peat profiles

Hg concentration in peat cores of the WSL are illustrated in Fig. 2, and primary data on soil chemical composition and Hg concentration are listed in Table S2 of the Supplement. The upper 0–20 cm layer is 2 to 3 times more enriched with Hg compared to the rest of the peat core in permafrost-affected sites (Khanymey, Pangody, and Tazovsky). This is not the case, however, for the sporadic-permafrost zone (Kogalym) and isolated-permafrost zone (Mukhrino), where a local maximum at ca. 35 cm depth was detected, but no enrichment of the upper 10–20 cm horizons occurred. In the permafrost-free site of the WSL (Plotnikovo, southern taiga), the Hg concentration profile in the peat was fairly constant, with a local minimum at 100 cm depth. The mean depth-integrated Hg concentrations in active-layer, permafrost, and mineral horizons are illustrated in Fig. 3 and summarized in Table 1. The latitudinal trend of Hg concentration in peat consists of a systematic increase northward, both in permafrost and active peat layers. The dominant ground vegetation (lichens) analyzed at five sites out of six (Plotnikovo, Kogalym, Khanymey, Pangody and Tazovsky) did not show significantly different (Mann–Whitney U test) Hg concentrations relative to the peat cores (Fig. 3). Mercury concentrations in the six WSL peat cores ranged from 7 to $284\,\mathrm{ng\,g^{-1}}$, with a median (± IQR) of $67 \pm 57\,\mathrm{ng\,g^{-1}}$. The Hg concentration in the thawed, active layer was generally comparable to that in the frozen layer, supported by a Mann–Whitney test, which did not show a significant difference in Hg concentration between frozen and thawed peat in all permafrost-affected sites. Within the latitudinal transect from south to north, the Hg concentrations in peat are higher (Plotnikovo, Kogalym, Khanymey, Pangody) or comparable (Tazovsky) to those in the mineral horizons.

The ratio of Hg : C (R_{HgC}, $\mu\mathrm{g\,g^{-1}}$, corresponding to $\mathrm{Gg\,Pg^{-1}}$) ranged between 0.05 and 2.0 over the peat columns and was 5 to 10 times higher in mineral horizons compared to frozen peat and active layers (Fig. 4). The R_{HgC} in the active layer and in the mineral horizons increased 3-fold from the south (56° N) to the north (67° N). In the frozen peat horizon, the R_{HgC} ratio increased 2-fold from the sporadic- and isolated- to the continuous-permafrost zone.

3.2 Regional and total pools of Hg in the WSL peat and mineral layers

The mass of Hg per area of soil in the active and frozen peat layer as well as in the top 30 cm of frozen mineral horizons of the six studied WSL peat profiles was calculated by

Table 1. Mean (±SD) concentrations and stocks of C and Hg in six studied sites in the Western Siberian Lowland (WSL) peat bogs.

Horizons	C, %	Hg, ng g^{-1}	kg C m^{-2}	mg Hg m^{-2}	R_{HgC} (Gg Pg^{-1})
Plotnikovo (Pl), southern taiga, 56.9° N*					
ALT (0–140 cm)	45 ± 2	36 ± 12	24	2.8	0.08 ± 0.03
Mineral (140–150 cm)	13	53	23	9.0	0.40
Total (150 cm)	43 ± 8	37 ± 12	47	11.8	0.10 ± 0.09
0–30 cm	44 ± 2	44 ± 5	3	0.3	0.10 ± 0.01
0–100 cm	45 ± 2	36 ± 10	9	0.8	0.08 ± 0.02
Mukhrino (Mh), middle taiga, 60.9° N*					
ALT (0–360 cm)	53 ± 7	26 ± 13	67	4.3	0.05 ± 0.03
Mineral (360–380 cm)	15 ± 19	24 ± 19	51	8.3	0.46 ± 0.46
Total (380 cm)	51 ± 10	26 ± 19	118	12.6	0.07 ± 0.12
0–30 cm	50 ± 0.4	29 ± 7	4	0.3	0.06 ± 0.02
0–100 cm	52 ± 5	32 ± 17	18	1.3	0.06 ± 0.04
Kogalym (Kg), northern taiga, 62.3° N*					
ALT (0–175 cm)	48 ± 4	48 ± 30	93	8.7	0.10 ± 0.06
Mineral (175–190 cm)	10 ± 13	12 ± 10	17	2.3	0.34 ± 0.36
Total (190 cm)	45 ± 12	45 ± 30	110	11	0.12 ± 0.12
0–30 cm	45 ± 1	65 ± 19	3	0.5	0.14 ± 0.04
0–100 cm	47 ± 2	49 ± 34	38	3	0.11 ± 0.07
Khanymey (Kh), northern taiga, 63.8° N					
ALT (0–34 cm)	44 ± 2	64 ± 43	17	2.1	0.15 ± 0.10
PF1 (34–100 cm)	50 ± 2	47 ± 13	78	7.6	0.09 ± 0.02
PF2 (34–138 cm)	48 ± 6	47 ± 11	119	11.8	0.10 ± 0.02
Mineral (138–147 cm)	1 ± 1	4 ± 1	2	0.5	0.31 ± 0.13
Total (147 cm)	42 ± 16	47 ± 28	138	14.4	0.13 ± 0.09
0–30 cm	43 ± 1	71 ± 46	13	1.8	0.17 ± 0.11
0–100 cm	47 ± 4	54 ± 29	95	9.6	0.12 ± 0.07
Pangody (Pg), forest tundra, 65.9° N					
ALT (0–40 cm)	50 ± 4	78 ± 25	38	5.3	0.16 ± 0.07
PF1 (40–100 cm)	53 ± 4	61 ± 25	54	6.6	0.11 ± 0.04
PF2 (40–155 cm)	48 ± 10	67 ± 23	78	11.0	0.15 ± 0.07
Mineral (155–185 cm)	3 ± 1	24 ± 11	15	12.5	0.88 ± 0.28
Total (185 cm)	41 ± 19	62 ± 28	130	28.8	0.27 ± 0.30
0–30 cm	50 ± 5	83 ± 26	26	4.0	0.17 ± 0.07
0–100 cm	52 ± 4	68 ± 25	92	11.9	0.13 ± 0.06
Tazovsky (Tz), southern tundra, 67.4° N					
ALT (0–40 cm)	49 ± 3	186 ± 110	22	7.4	0.38 ± 0.20
PF1 (40–100 cm)	46 ± 3	109 ± 28	27	6.3	0.23 ± 0.06
PF2 (40–380 cm)	47 ± 4	104 ± 39	156	35.0	0.22 ± 0.08
Mineral (380–405 cm)	14 ± 5	152 ± 65	60	64.7	1.24 ± 0.66
Total (405 cm)	45 ± 9	115 ± 57	238	107.0	0.30 ± 0.31
0–30 cm	49 ± 4	209 ± 120	16	6.0	0.42 ± 0.21
0–100 cm	47 ± 3	140 ± 80	48	13.7	0.29 ± 0.15

ALT is active-layer thickness; PF1 is frozen peat (ALT − 100 cm); PF2 is frozen peat (ALT to mineral layer); "mineral" is mineral layer; "total" is total Hg content averaged over full sampled depth. * In the permafrost-free zone, the ALT extends from the surface to the mineral layer.

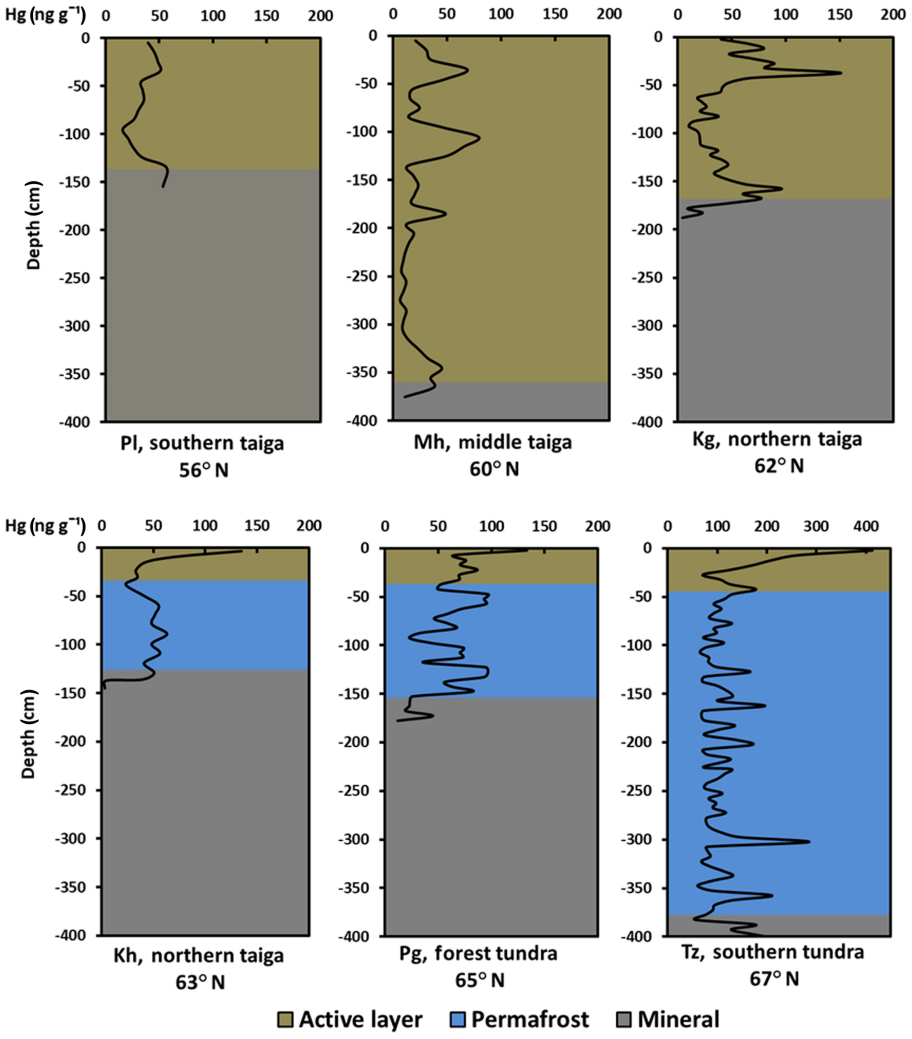

Figure 2. Vertical-depth profile distribution of total Hg (THg) in six peat cores across a 1700 km latitudinal transect of the WSL. Site location and physiogeographical parameters are shown in Fig. 1 and Table S1.

multiplying bulk soil peat and mineral layer densities (ranging from 0.01 to 0.38 g cm^{-3}; Table S2) by Hg concentration and integrating over the corresponding depths. The difference between surface-area-normalized Hg stock systematically increased from south to north (ca. 0.3 to 6.0 and ca. 0.8 to 13.7 mg Hg m^{-2}, in the 0–30 and the 0–100 cm peat layer, respectively; Fig. 5a). This northward increase was most pronounced for the active layer, less evident for frozen peat, and insignificant for the upper 30 cm of mineral horizon located under the peat (Fig. 5b). Taking into account the proportion of bogs (peatlands) in each zone (1° latitudinal grid) from Sheng et al. (2004), we calculated the pool of Hg in permafrost-free and permafrost-affected WSL peatlands (Fig. 6). The total pool of Hg in the 0–100 cm layer of peat bogs exhibits a maximum (356–580 Mg) in the discontinuous-permafrost zone.

We estimate the total organic soil Hg pool in the WSL from the Hg stock (mg Hg m^{-2} over 0–100 cm depth) for permafrost and permafrost-free zones (Fig. 7a), extrapolated to the full average thickness of peat in the WSL (280 cm; Sheng et al., 2004) and assuming that Hg concentration in the upper 0–100 cm peat layer is the same as in 100–280 cm of peat. We then multiplied this Hg concentration in the upper 0–100 cm peat layer by the area of the bogs in each latitudinal grid (° S, m^2) as shown in Fig. 7b. This yields 1.7 Gg Hg in the permafrost-free zone and 7.6 Gg Hg in the permafrost-bearing zone, with a total Hg pool of 9.3 Gg in the WSL. For this calculation we did not take into account the mineral horizons, and we used variable active-layer thickness across the latitudinal gradient of the WSL, as estimated at our sampling sites (Table S1). The amount of Hg in the permafrost-bearing zone within the active (unfrozen) peat layer (0–160 cm in the south and 0–20 cm in the north) of the WSL is 2.0 Gg, and that in the frozen (160–280 cm in the south and 20–280 cm in the north) layer is 5.6 Gg.

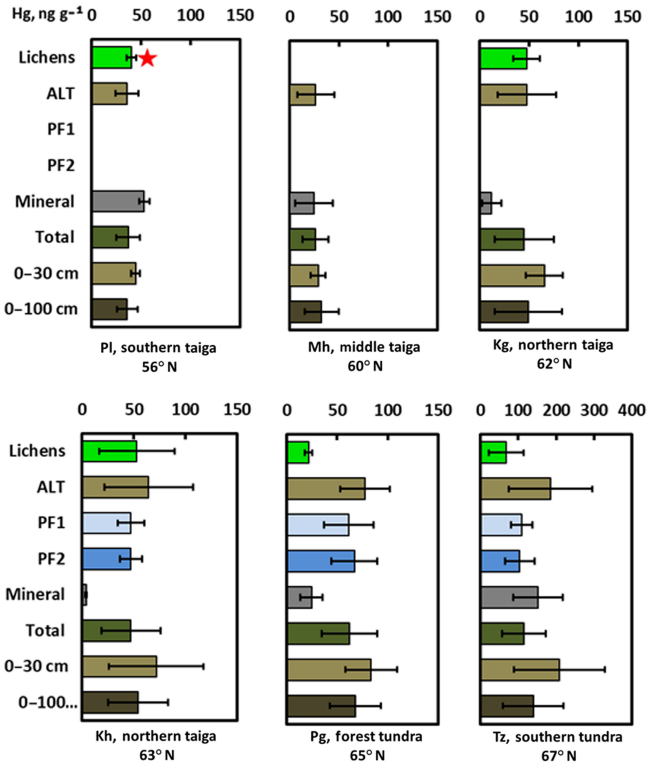

Figure 3. Mean (±SD) depth-integrated Hg concentrations in peat columns and mineral layers of six studied sites. The red asterisk represents the data from Lyapina et al. (2009). ALT is active-layer thickness; PF1 is frozen peat (ALT − 100 cm); PF2 is frozen peat (ALT to mineral layer); "mineral" is mineral layer; "total" is total Hg content averaged over the full sampled depth. * In the permafrost-free zone, the ALT extends from the surface to the mineral layer.

Alternatively, to calculate the total pool of Hg in WSL bogs, we used the R_{HgC} inferred from our data across the gradient of permafrost and biomes (Table 1). Taking into account the C pool in the WSL (70.2 Pg C of the 0–280 cm depth layer; Sheng et al., 2004) and the median R_{HgC} of 0.133 Gg Pg^{-1} in the WSL, we calculated Hg for the full depth of the peat layer in each zone. This also gives 9.3 Gg Hg for a total area of 592 440 km^2.

3.3 Correlation of Hg with other elements in the peat cores

Spearman rank order correlations $R_{Spearman}$ of Hg with other elements demonstrated significant positive relationships ($R_{Spearman} > 0.60$; $p < 0.05$) with K, Rb, Cs, P, As, W, V, Cr, and Cu in the active (unfrozen) layer (Table S3 of the Supplement). However, these relationships were less pronounced in the frozen peat, where only Mg, Ca, Sr, Mn, N, P, As, Cu, Ni, Sb, and some rare earth elements (REEs) demonstrated minor ($0.40 < R_{Spearman} < 0.55$) positive correlations with Hg. Finally, in the mineral layer, significant ($R_{Spearman} > 0.70$) positive correlations of Hg were observed with Li, Ca, Sr, P, N, Mn, Ni, Co, Cr, and Cd. A positive ($R_{Spearman} = 0.60$) relationship between Hg and C was observed in mineral horizons, whereas no correlation was detected in both frozen and thawed peat. This is consistent with some studies of peat soil in Brazil (Roulet et al., 1998) and Arctic tundra soils (Olson et al., 2018). At the same time, there was a positive correlation of Hg with nitrogen (N) in the active layer, frozen peat, and mineral horizons ($R_{Spearman} =$ 0.50, 0.47, and 0.75, respectively). Stronger and more stable correlation of Hg with N compared to C was also noted by Roulet (2000).

4 Discussion

4.1 Hg association with other elements in peat

Stronger accumulation of Hg relative to C in mineral horizons in the north (Tazovsky, Fig. 4) may be linked to the clay nature of mineral layers (Roulet et al., 1998; Baptista-Salazar et al., 2017) in these regions (Table S1) but also to the presence of specific host phases of Hg (see examples of peat minerals in Rudmin et al., 2018). Dissolved oxygen measurements in soil porewaters at the Tazovsky site indicate that mineral Gleysols and peat Histosols, which often overlay former lake sediments, are anoxic (Raudina et al., 2017; Loiko et al., 2019). The Hg host phases in these soils are therefore likely sulfide minerals. Indeed, known Hg carriers in peat deposits are Fe and Zn sulfide minerals or organic-bound sulfide functional groups (Smieja-Król et al., 2010; Prietzel et al., 2009; Skyllberg et al., 2003, Bates et al., 1998; Steinmann and Shotyk, 1997).

In the peat active layer, Hg was positively correlated with K, Rb, Cs, P, As, V, Cr, and Cu (Table S3). In the frozen part of the peat core, Hg was positively correlated with Ca, N, Mn, Sr, Mg, P (Table S3). Indeed, atmospheric particles in snow across the WSL exhibit strong enrichment in Mo, W, As, Sb, Ni, Cu, Zn, Cd, Pb, Mg, Ca, and Na (Shevchenko et al., 2017). The strong positive correlation of Hg with these elements in peat soils of the WSL suggests a common atmospheric origin. Note, however, that the cited elements deposit with particles, rainfall, and snowfall, whereas atmospheric Hg transfer to peat occurs mainly via the vegetation pump, with tundra and taiga vegetation actively taking up atmospheric gaseous Hg^0 through foliage (Obrist et al., 2017; Jiskra et al., 2018).

4.2 Estimating the pan-Arctic permafrost soil Hg pool

A recent study used a median R_{HgC} value of 1.6 Gg Pg^{-1}, observed mainly in mineral soil samples (median soil organic carbon, SOC, of 3 %, IQR is 1.7 % to 8.7 %) along a transect in Alaska, to estimate a pan-Arctic permafrost soil Hg pool of 755 ± 427 Gg in the upper 0–100 cm and 1656 ± 962 Gg in the upper 0–300 cm, respectively (Schus-

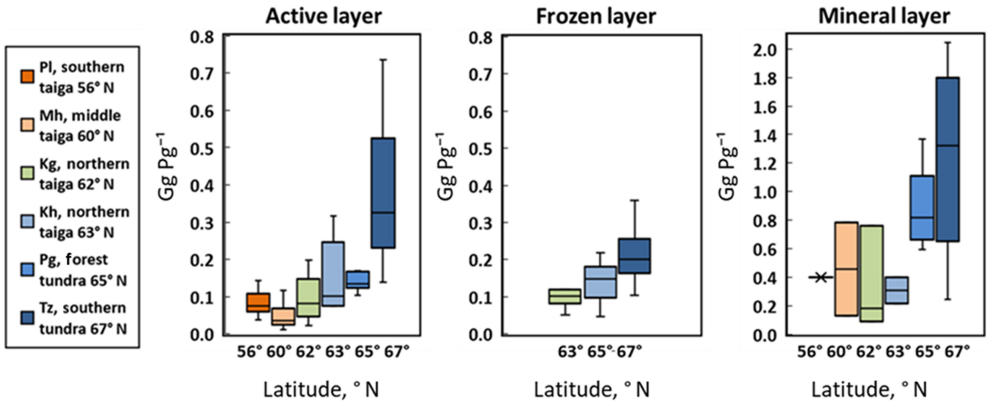

Figure 4. The ratio Hg : C (Gg Pg^{-1}; median ± IQR) in the active layer, frozen peat, and mineral horizons across the WSL latitudinal transect.

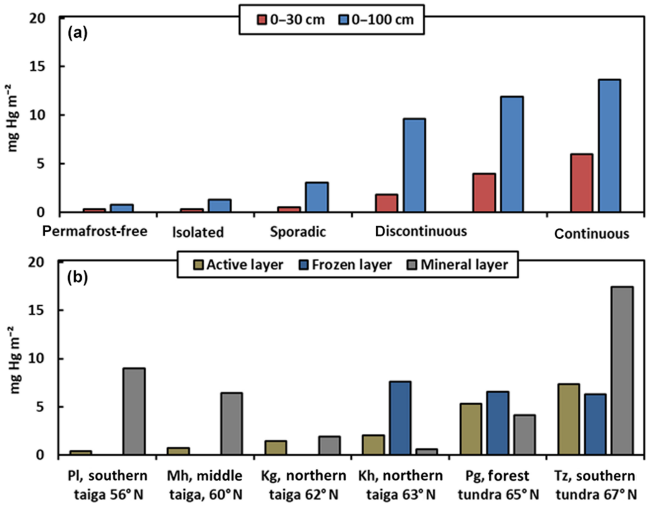

Figure 5. Latitudinal variation in WSL soil Hg storage (mg Hg m^{-2}) in the 0–30 and 0–100 cm peat layer **(a)** and in the active, frozen, and mineral layers **(b)**. In the permafrost-free zone, the first 40 cm were used to calculate Hg storage in the active layer. The permafrost peat layer is fixed from the lower boundary of the active (unfrozen) layer down to 100 cm. Finally, for the mineral layer we considered only the first 10 cm below peat deposits across the full latitudinal gradient of the WSL peatland.

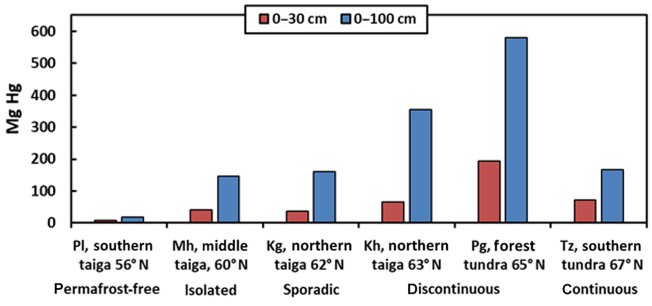

Figure 6. Total depth-integrated pools of Hg mass (Mg) in the upper 0–30 and 0–100 cm (red and blue columns, respectively) of WSL frozen peatlands in each permafrost zone. The stocks are calculated assuming the areal proportion of bogs from the landscape inventory across the WSL (Sheng et al., 2004).

ter et al., 2018). In the case of Western Siberia, this high R_{HgC} value overestimates the Hg pool 12-fold given that the median R_{HgC} in WSL peat is only 0.13 ± 0.12 Gg Pg^{-1} (median ± IQR) (Table 1, Fig. 4). The extrapolation based on Alaskan R_{HgC} for the whole Northern Hemisphere permafrost region also suggests that the WSL contains large amounts of Hg in the upper 0–30 cm (20–40 mg Hg m^{-2}) and in the upper 0–100 cm (40–80 mg Hg m^{-2}). These numbers are much higher than the direct measurements in this study: 0.3 mg Hg m^{-2} in the 0–30 cm layer and 0.8–1.3 mg Hg m^{-2} in the 0–100 cm layer in the permafrost-free zone (Plotnikovo and Mukhrino sites), 0.5 mg Hg m^{-2} in the 0–30 cm layer and 3.0 mg Hg m^{-2} in the 0–100 cm layer in the sporadic zone (Kogalym site), 1.8–4.0 mg Hg m^{-2} in the 0–30 cm layer and 9.6–11.9 mg Hg m^{-2} in the 0–100 cm layer in the continuous- to discontinuous-permafrost zone (Khanymey and Pangody sites), and 6.0 mg Hg m^{-2} in the 0–30 cm layer and 13.7 mg Hg m^{-2} in the 0–100 cm layer in the continuous-permafrost zone (Tazovsky). It is worth noting that the recent data of Talbot et al. (2017) for Ontario (Canada) bogs (surface area: 1 133 990 km^2; 18.8 Gg Hg at a depth of 277 ± 123 cm) are consistent with the results of the present study in the WSL (9.3 Gg Hg for 592 440 km^2 at a depth of 280 ± 100 cm).

A revised value of the Hg pool in the pan-Arctic permafrost soils was recently provided by Olson et al. (2018), who combined measured R_{HgC} values for Alaskan tundra soils (Dalton Highway, Noatak National Preserve, 8 Mile Lake Observatory) with literature data (Table S4) and derived R_{HgC} of 0.12 Gg Pg^{-1} for the 0–30 cm (organic) and 0.62 Gg Pg^{-1} for the 30–100 cm (mineral) layers. Note that Table 1 from Olson et al. (2018) has an incorrect organic soil R_{HgC} of 0.274 Gg Pg^{-1}, which should be

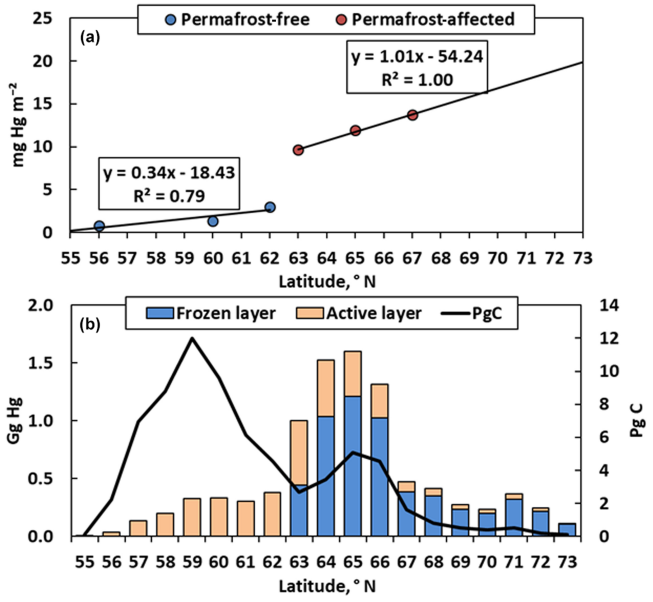

Figure 7. Estimated Hg storage (mg Hg m^{-2}) in the 0–100 cm soil layer of the WSL **(a)** and latitudinal distribution of the Hg pool (Gg) in active and frozen peat layers of the WSL **(b)**. The solid black line represents the WSL C pool (Pg) from Sheng et al. (2004).

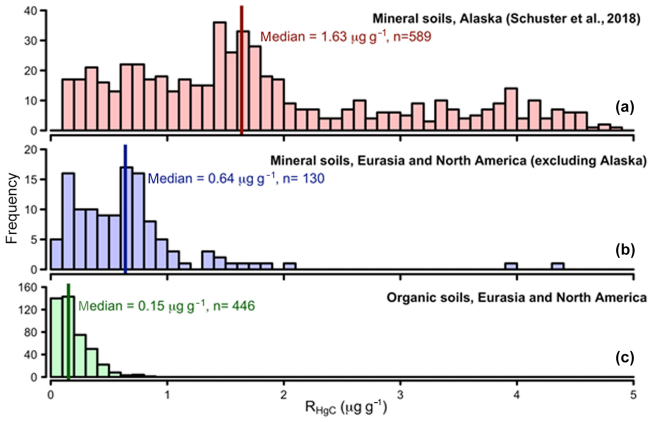

Figure 8. Histograms of published (Table S4) and WSL (this study) R_{HgC} data used for estimating the northern circumpolar permafrost region soil Hg pool: **(a)** Alaskan mineral soils (Schuster et al., 2018), **(b)** mineral soils from Eurasia and North America (excluding Alaska), and **(c)** organic soils from Eurasia and North America (including Alaska).

0.119 Gg Pg^{-1}; the typo did not affect their soil Hg budgets. Olson et al. (2018) estimate pan-Arctic permafrost soil Hg pools of 26 Gg (0–30 cm) and 158 Gg (30–100 cm), which when combined (184 Gg) is 4 times lower than the number of 755 Gg (0–100 cm) by Schuster et al. (2018). Both studies report R_{HgC} measurements from Alaskan soils due to relatively easy road access to the sampling sites along the Dalton Highway. The bedrock along the Dalton Highway contains relatively high geogenic Hg levels (mean concentration: 32 ng g^{-1}), resulting in a high geogenic contribution in mineral soils (39 % for B horizons and 20 % for A horizons; Obrist et al., 2017). It is clear that any upscaling calculation of pan-Arctic permafrost Hg depends critically on the R_{HgC} of the 0–30 and 30–100 cm peat layers as Eurasian sporadic to continuous permafrost represents 54 % of the northern soil C inventory (Table 2). We combined our new WSL data ($n = 202$) with literature data covering Russia ($n = 42$), Scandinavia ($n = 97$), Canada ($n = 122$), and Alaska ($n = 703$) to build a pan-Arctic database for R_{HgC} (Table S4). Setting Alaska aside, as a geographic region with high geogenic Hg, we find that Eurasian and North American (excluding Alaska) mineral (< 20 % SOC) soil R_{HgC} was lower ($\mu = 0.67$ Gg Pg^{-1}, median = 0.64 Gg Pg^{-1}, IQR is 0.33 to 0.79 Gg Pg^{-1}, $n = 130$) than R_{HgC} reported for mineral soils along the Dalton Highway in Alaska (median = 1.64 Gg Pg^{-1}, IQR is 0.91 to 2.93 Gg Pg^{-1}, $n = 589$; Schuster et al., 2018; Fig. 8). The R_{HgC} in organic soils (> 20 % SOC, including data from Alaska) was approximately 4 times lower ($\mu = 0.19$ Gg Pg^{-1}, median = 0.15 Gg Pg^{-1}, IQR is 0.09 to 0.25 Gg Pg^{-1}, $n = 446$) than that in mineral soils of Eurasia and North America (excluding Alaska) (Fig. 8), which is consistent with the observed difference in WSL mineral and organic soils. Higher R_{HgC} observed in mineral soils may originate from a contribution of geogenic Hg from the weathered bedrock (independent of C stock) and/or a higher mineralization rate of C (C loss is stronger than Hg loss) in predominantly oxic mineral soils compared to anoxic peat soils.

In Table 2 we revisit the full 0–300 cm pan-Arctic permafrost soil Hg inventory. For this, we used Eurasian and North American (excluding Alaska) R_{HgC} based on the literature data compilations of Olson et al. (2018) and Schuster et al. (2018) and our observed WSL R_{HgC} for Eurasia, multiplied by estimated organic C pools for the northern permafrost region covering 17.8×10^6 km^2 from Hugelius et al. (2014). The systematic underestimation made by neglecting high R_{HgC} in Alaskan mineral soils is small, on the order of 2.5 Gg Hg, due to a relatively small Alaskan C pool of 2.6 Pg C (Tarnocai et al., 2009). We estimate the pan-Arctic permafrost soil Hg pool to be 72 Gg (39–91 Gg, IQR) in the upper 30 cm, 240 Gg (110–336 Gg) in the upper 1 m, and 597 Gg (384–750 Gg) in the upper 3 m (Table 3). Note that our revised value in the 0–1 m range (240 Gg) is similar to that of Olson et al. (2018; 184 Gg) but sizably lower than that of Schuster et al. (2018; 755 Gg). We find that Hg stocks in organic soils (> 20 % SOC) represent 52 % and 21 % of the total Hg stock in the 0–30 and 0–100 cm depth range, respectively (Table 2). The rest of the pan-Arctic Hg is associated with C in mineral soils (< 20 % SOC) for which relatively sparse data exist ($n = 131$). In particular, Turbel and Orthel mineral soils, which are estimated to contain 49 % to 62 % of total Arctic C, respectively (Hugelius et al., 2014),

Table 2. Estimated pan-Arctic permafrost soil Hg inventory (Gg) for different depth ranges down to 300 cm. Hg pool uncertainties are reported as the interquartile range (IQR), i.e., the 25th to 75th percentiles of the Hg pool distribution estimates by a Monte Carlo method. Soil organic carbon (SOC) pools are from Hugelius et al. (2014).

Depth range	Soils	SOC (Pg)	Hg pool (Pg)	IQR		% of total
0–30 cm	Organic (> 20 % SOC)	172	35	13	45	48
	Mineral (< 20 % SOC)	45	37	15	47	52
	Total	217	72	39	91	
0–100 cm	Organic (> 20 % SOC)	253	50	26	65	21
	Mineral (< 20 % SOC)	219	191	59	287	79
	Total	472	240	110	336	
0–200 cm	Organic (> 20 % SOC)	366	72	44	92	16
	Mineral (< 20 % SOC)	461	392	196	529	84
	Total	827	464	269	601	
0–300 cm	Organic (> 20 % SOC)	427	85	55	106	14
	Mineral (< 20 % SOC)	607	512	300	666	86
	Total	1034	597	384	750	

and 36 % to 85 % of Hg, respectively, at the various depth intervals need to be further investigated.

4.3 Estimating Earth's global soil (0–30 cm) Hg pool

To assess Earth's global soil Hg pool, we combined the more detailed Arctic pool estimate (separating organic and mineral soils) with a more basic approach for the other climate zones, where we derived bulk R_{HgC}'s for the 0–30 cm surface soils based on published literature data. The core dataset for this analysis was the global literature compilation by Schuster et al. (2018) with 11 000 data points, of which 6224 data points were from the 0–30 cm range. This global dataset was complemented by soil Hg data from the boreal (Olson et al., 2018) and tropical (Campbell et al., 2003; Almeida, 2005; Almeida et al., 2005; Melendez-Perez et al., 2014) zones. The R_{HgC}'s for each climate zone (Arctic, boreal, temperate, subtropical, and tropical) were then multiplied by the respective C stock estimates from the global soil organic carbon map (FAO and ITPS, 2018). The R_{HgC} of all 0 to 30 cm soil data increases from cold climate zones to warmer climate, from 0.36 Gg Pg^{-1} for Arctic soils (excluding Alaska) to 1.8 Gg Pg^{-1} in subtropical and tropical soils (Fig. 9, Table 4). This latitudinal trend in R_{HgC} likely reflects a combination of low C mineralization rates in colder northern soils and additional Hg sorption to Fe(oxi)hydroxides in old tropical soils. Taking into account the variation in R_{HgC} and C stocks across the climate zones, we estimate a global Hg stock of 1086 Gg (852–1265 Gg, IQR) for the top 0–30 cm (Table 4). Previous global Hg soil pool estimates vary between 232 and 1150 Gg (Selin et al., 2008; Smith-Downey et al., 2010; Amos et al., 2014, 2015; Hararuk et al., 2013; Wang et al., 2019). Schuster et al. (2018) concluded that Arctic permafrost soils store nearly twice the amount of Hg as all other soils, the ocean, and the atmosphere combined, but in doing so they compared different depth ranges for global (typically 0–15 or 0–20 cm) and Arctic soil estimates (0–300 cm). Our revised estimate of the pan-Arctic permafrost and global soil pool suggests that, for a similar depth range of 0–30 cm, permafrost soils contain 7 % (72 Gg) of the global soil Hg pool (1086 Gg).

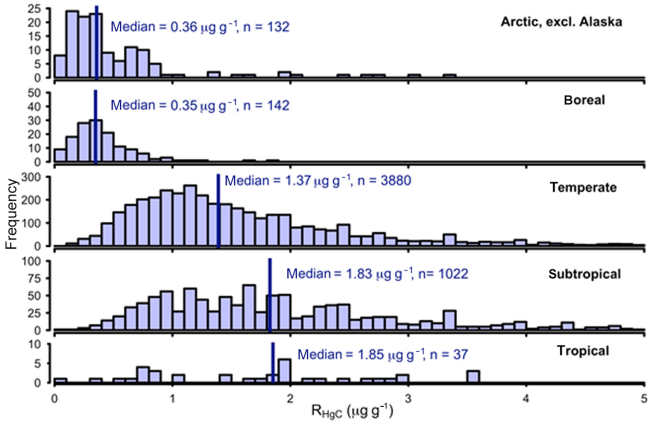

Figure 9. Histograms and median R_{HgC} for the 0–30 cm soil interval for different global climate zones.

4.4 Northern soil Hg sequestration and Hg loss

Olson et al. (2018) recognized that the large 0–100 cm northern soil Hg pool is the result of thousands of years of net atmospheric Hg deposition. The latitudinal trend of northward-

Table 3. Comparison of estimated pan-Arctic permafrost soil Hg pools by different studies.

Depth range	Hugelius et al. (2014)		Schuster et al. (2018)		Olson et al. (2018)		This study	
	SOC (Pg)	95 % CI (Pg)	Hg Pool (Gg)	95 % CI (Gg)	Hg Pool (Gg)	25 % CI (Gg)	Hg Pool (Gg)	IQR (Gg)
0–30 cm	217	12	347	±196	26	21–42*	72	39–91
0–100 cm	472	27	755	±301	184	136–274*	240	110–336
0–200 cm	827	108	1323	±764			464	269–601
0–300 cm	1034	150	1656	±962			597	384–750

* Confidence interval (CI) corresponding to the 37.5th to 62.5th percentile.

Table 4. Estimated soil Hg pool (0 to 30 cm interval) for different climate zones based on reported R_{HgC} and carbon pools. Hg pool uncertainties are reported as the interquartile range (IQR), i.e., the 25th to 75th percentiles of the Hg pool distribution estimates by a Monte Carlo method.

Climate zone	C pool (Pg)	Median R_{HgC} (Gg Pg^{-1})	Mean R_{HgC} (Gg Pg^{-1})	Hg pool (Gg)	IQR (Gg)
Tropics[a]	208	1.85	2.14	446	268–556
Subtropics[a]	102	1.83	2.13	217	128–271
Temperate[a]	191	1.37	1.55	296	183–366
Boreal[a]	140	0.35	0.41	55	35–67
Arctic[b]	217[c]	(0.15, 0.64)	(0.19, 0.67)	72	39–91
Total	858			1086	852–1265

[a] Carbon pools are from FAO and ITPS (2018). [b] The Arctic R_{HgC} and Hg pool are from Table 2. [c] The Arctic carbon pool is from Hugelius et al. (2014).

increasing peat Hg concentration in the WSL (Figs. 4, 5) illustrates that this net Hg deposition is a fine balance between the vegetation Hg pump, which sequesters Hg^0 in soils via foliar uptake and litterfall, and Hg^0 emission during biomass degradation. Annual gross Hg sequestration by vegetation via the vegetation pump likely scales with primary productivity and therefore decreases northward as insolation and growing season decrease. However, in the north, degradation rates of vegetation biomass are lower than in the south: the moss biomass loss during decomposition in the forest tundra zone (5–6 % over first year and 10–12 % over 2 years) is lower than that in the southern taiga (10–20 % over first year and 20–40 % over 2 years) based on in situ biomass degradation experiments across the WSL gradient of biomes (Vishnyakova and Mironycheva-Tokareva, 2018). The net result is a higher preservation of soil Hg in the north, where less emission of Hg^0 during plant decay occurs. The dependence of this balance between Hg^0 sequestration and Hg^0 re-emission on climate qualitatively explains the contrasting observations made in Toolik (AK, USA, 68° N; MAAT: −7 °C; Obrist et al., 2017) and Degerö Stormyr (Sweden, 64° N; MAAT: 2 °C; Osterwalder et al., 2018). At Toolik, net Hg^0 deposition by vegetation and soil uptake occurs on an annual basis, whereas at Degerö Stormyr higher temperatures result in net annual Hg^0 emission. More research is needed to quantify the climate dependence of Hg^0 sequestration (as soil Hg^{II}) and Hg^0 re-emission before we can predict and model northern soil Hg loss to the atmosphere due to global warming trajectories.

5 Conclusions

Western Siberian peatlands contain a large amount of Hg in frozen and thawed peat; the lateral pools of peat palsa bogs range from between 1 and 2 mg Hg m^{-2} in the south to between 10 and 15 mg Hg m^{-2} in the north. This northward increase of Hg concentration and pools can be explained by better preservation of organic-bound Hg, i.e., lower Hg re-emissions, due to colder temperatures and a shorter active period in the continuous-permafrost zone compared to the discontinuous and sporadic zones. We revisited the full 0–300 cm pan-Arctic permafrost soil Hg inventory, based on published R_{HgC} and our observed WSL R_{HgC}, together with estimated pan-Arctic permafrost soil organic C pools for 0–300 cm from Hugelius et al. (2014). We estimate the 0–300 cm pan-Arctic permafrost soil Hg inventory to be 597 Gg (384–750 Gg, IQR), which is 3 times lower than a previous estimate of 1656 ± 962 Gg Hg for the same depth range (Schuster et al., 2018). We estimate the global soil Hg pool to be 1086 Gg for the 0–30 cm depth range. The permafrost

Hg pool for the same 0–30 cm depth range is 72 Gg, and while large compared to the 3 Gg of Hg residing in the Arctic Ocean (Soerensen et al., 2016), it represents only 7 % of the global soil Hg pool.

We document large regional differences in R_{HgC} driven by (1) different contributions of geogenic Hg in mineral soils, e.g., resulting in higher R_{HgC} in Alaska than in other areas of the pan-Arctic permafrost region, and (2) the stability of Hg with respect to emission from organic soils, e.g., resulting in a gradient with increasing R_{HgC} towards the north of the WSL. These systematic differences illustrate the limitations of the pool size estimation approach where C inventories are multiplied by average R_{HgC} values, and they emphasize the need for spatially resolved sampling and pool size estimates, similar to the pan-Arctic permafrost C pool estimates (Hugelius et al., 2014). In particular, to estimate the release of Hg to aquatic ecosystems, e.g., coastal erosion and transfer to rivers and Hg evasion to the atmosphere, spatially resolved Hg soil pools will be valuable.

Data availability. Hg and C concentration data of the WSL soil samples are available in the Supplement. A summary of pan-Arctic literature data is provided in the Supplement. The permafrost data from Schuster et al. (2018) and a global compilation of R_{HgC} data are available at https://agupubs.onlinelibrary.wiley.com/action/downloadSupplement?doi=10.1002/2017GL075571&file=grl56886-sup-0002-2017GL075571-ds01.csv and https://agupubs.onlinelibrary.wiley.com/action/downloadSupplement?doi=10.1002/2017GL075571&file=grl56886-sup-0003-2017GL075571-ds02.csv. The Arctic and boreal soil data from the Olson et al. (2018) study are available from the corresponding author upon request. Note that Table 1 from Olson et al. (2018) has an incorrect organic soil R_{HgC} of 0.274 Gg Pg^{-1}, which should be 0.119 Gg Pg^{-1}. The data from the tropical climate zone were compiled from original publications of Almeida (2005), Almeida et al. (2005), Campbell et al. (2003), and Melendez-Perez et al. (2014).

Supplement. The supplement related to this article is available online at: https://doi.org/10.5194/bg-17-3083-2020-supplement.

Author contributions. OSP and SVL designed the study. SVL, AGL, and NK performed field sampling. AGL and OSP did all laboratory analysis. MJ and JES did the northern soil and global soil Hg pool calculations. All authors contributed to the writing of the manuscript.

Competing interests. The authors declare that they have no conflict of interest.

Acknowledgements. We are thankful to Luiz D. Lacerda for sharing Hg and C data from Brazil.

Financial support. This research has been supported by the Russian Science Foundation (project no. 18-77-10045), Russian Fund for Basic Research (grant nos. 19-29-05209-mk and 19-55-15002-NCNI_a), the CNRS Chantier Arctique Français (via the PARCS project), and the European Commission, H2020 Research Infrastructures, ERA-PLANET (grant no. 689443), iGOSP and iCUPE programs. Martin Jiskra acknowledges funding by the Swiss National Science Foundation (grant no. PZ00P2_174101).

Review statement. This paper was edited by Andreas Richter and reviewed by two anonymous referees.

References

Almeida, M. D.: Biogeoquímica de mercúrio na interface solo-atmosfera na Amazônia, PhD thesis, Univsidade Federal Fluminense, Niterói, Brazil, 221 pp., 2005.

Almeida, M. D., Lacerda, L. D., Bastos, W. R., and Herrmann, J. C.: Mercury loss from soils following conversion from forest to pasture in Rondônia, Western Amazon, Brazil, Environ. Pollut., 137, 179–186, https://doi.org/10.1016/j.envpol.2005.02.026, 2005.

AMAP: AMAP Assessment 2011: Mercury in the Arctic. Arctic Monitoring and Assessment Programme (AMAP), Oslo, Norway, xiv + 193 pp., https://www.amap.no/documents/doc/amap-assessment-2011-mercury-in-the-arctic/90 (last access: 15 June 2020), 2011.

Amos, H. M., Jacob, D. J., Kocman, D., Horowitz, H. M., Zhang, Y., Dutkiewicz, S., Horvat, M., Corbitt, E. S., Krabbenhoft, D. P., and Sunderland, E. M.: Global biogeochemical implications of mercury discharges from rivers and sediment burial, Environ. Sci. Technol., 48, 9514–9522, https://doi.org/10.1021/es502134t, 2014.

Amos, H. M., Sonke, J. E., Obrist, D., Robins, N., Hagan, N., Horowitz, H. M., Mason, R. P., Witt, M., Hedgecock, I. M., Corbitt, E. S., and Sunderland, E. M.: Observational and modeling constraints on global anthropogenic enrichment of mercury, Environ. Sci. Technol., 49, 4036–4047, https://doi.org/10.1021/es5058665, 2015.

Bailey, E. A., Gray, J. E., and Theodorakos, P. M.: Mercury in vegetation and soils at abandoned mercury mines in southwestern Alaska, USA, Geochem.-Explor. Env. A., 2, 275–285, https://doi.org/10.1144/1467-787302-032, 2002.

Baptista-Salazar, C., Richard, J. H., Horf, M., Rejc, M., Gosar, M., and Biester, H.: Grain-size dependence of mercury speciation in river suspended matter, sediments and soils in a mercury mining area at varying hydrological conditions, Appl. Geochem., 81, 132–142, https://doi.org/10.1016/j.apgeochem.2017.04.006, 2017.

Bates, A. L., Spiker, E. C., and Holmes, C. W.: Speciation and isotopic composition of sedimentary sulfur in the Everglades, Florida, USA, Chem. Geol., 146, 155–170, https://doi.org/10.1016/S0009-2541(98)00008-4, 1998.

Brown, J., Ferrians Jr., O. J., Heginbottom, J. A., and Melnikov, E. S.: Circum-arctic map of permafrost and ground ice conditions, National Snow and Ice Data Center, Digital media, Boulder, CO 80309-0449 USA, 1998, revised February 2001.

Campbell, L. M., Hecky, R. E., Muggide, R., Dixon, D. G., and Ramlal, P. S.: Variation and distribution of total mercury in water, sediment and soil from northern Lake Victoria, East Africa, Biogeochemistry, 65, 195–211, https://doi.org/10.1023/A:1026058417584, 2003.

Dastoor, A. P. and Durnford, D. A.: Arctic Ocean: Is It a Sink or a Source of Atmospheric Mercury?, Environ. Sci. Technol., 48, 1707–1717, https://doi.org/10.1021/es404473e, 2014.

Fahnestock, M. F., Bryce, J. G., McCalley, C. K., Montesdeoca, M., Bai, S., Li, Y., Driscoll, C. T., Crill, P. M., Rich, V. I., and Varner, R. K.: Mercury reallocation in thawing subarctic peatlands, Geochem. Perspect. Lett., 6, 33–38, https://doi.org/10.7185/geochemlet.1922, 2019.

FAO and ITPS: Global Soil Organic Carbon Map (GSOCmap), Technical Report, Rome, 162 pp., 2018.

Fisher, J. A., Jacob, D. J., Soerensen, A. L., Amos, H. M., Steffen, A., and Sunderland, E. M.: Riverine source of Arctic Ocean mercury inferred from atmospheric observations, Nat. Geosci., 5, 499–504, https://doi.org/10.1038/ngeo1478, 2012.

Golovatskaya, E. A. and Lyapina, E. E.: Distribution of total mercury in peat soil profiles in West Siberia, Contemp. Probl. Ecol., 2, 156–161, https://doi.org/10.1134/S199542550902012X, 2009.

Hararuk, O., Obrist, D., and Luo, Y.: Modelling the sensitivity of soil mercury storage to climate-induced changes in soil carbon pools, Biogeosciences, 10, 2393–2407, https://doi.org/10.5194/bg-10-2393-2013, 2013.

Hugelius, G., Strauss, J., Zubrzycki, S., Harden, J. W., Schuur, E. A. G., Ping, C.-L., Schirrmeister, L., Grosse, G., Michaelson, G. J., Koven, C. D., O'Donnell, J. A., Elberling, B., Mishra, U., Camill, P., Yu, Z., Palmtag, J., and Kuhry, P.: Estimated stocks of circumpolar permafrost carbon with quantified uncertainty ranges and identified data gaps, Biogeosciences, 11, 6573–6593, https://doi.org/10.5194/bg-11-6573-2014, 2014.

Jensen, A. and Jensen, A.: Historical deposition rates of mercury in scandinavia estimated by dating and measurement of mercury in cores of peat bogs, Water Air Soil Pollut., 56, 769–777, https://doi.org/10.1007/BF00342315, 1991.

Jiskra, M., Sonke, J. E., Obrist, D., Bieser, J., Ebinghaus, R., Myhre, C. L., Pfaffhuber, K. A., Wängberg, I., Kyllönen, K., Worthy, D., Martin, L. G., Labuschagne, C., Mkololo, T., Ramonet, M., Magand, O., and Dommergue, A.: A vegetation control on seasonal variations in global atmospheric mercury concentrations, Nat. Geosci., 11, 244–250, https://doi.org/10.1038/s41561-018-0078-8, 2018.

Jiskra, M., Sonke, J. E., Agnan, Y., Helmig, D., and Obrist, D.: Insights from mercury stable isotopes on terrestrialatmosphere exchange of Hg(0) in the Arctic tundra, Biogeosciences, 16, 4051–4064, https://doi.org/10.5194/bg-16-4051-2019, 2019.

Kremenetski, K. V., Velichko, A. A., Borisova, O. K., MacDonald, G. M., Smith, L. C., Frey, K. E., and Orlova, L. A.: Peatlands of the Western Siberian lowlands: Current knowledge on zonation, carbon content and Late Quaternary history, Quaternary Sci. Rev., 22, 703–723, https://doi.org/10.1016/S0277-3791(02)00196-8, 2003.

Kurina, I. V. and Veretennikova, E. E.: Impact of climate change of the Holocene on the development of the ridge-hollow swamp complex of Western Siberia, Izvestiya Rossiiskoi Akademii Nauk, Seriya Geograficheskaya, 2, 74–87, https://doi.org/10.15356/0373-2444-2015-2-74-87, 2015 (in Russian).

Kurina, I. V., Veretennikova, E. E., Il'ina, A. A., Dyukarev, E. A., Golovatskaya, E. A., and Smirnov, S. V.: Reconstruction of conditions of formation of the eutrophic peatland deposits in south of the taiga zone of Western Siberia, Izvestiya Rossiiskoi Akademii Nauk, Seriya Geograficheskaya, 4, 66–76, https://doi.org/10.1134/S2587556618040106, 2018.

Lim, A. G., Sonke, J. E., Krickov, I. V., Manasypov, R. M., Loiko, S. V., and Pokrovsky, O. S.: Enhanced particulate Hg export at the permafrost boundary, western Siberia, Environ. Pollut., 254, 113083, https://doi.org/10.1016/j.envpol.2019.113083, 2019.

Loiko, S., Raudina, T., Lim, A., Kuzmina, D., Kulizhskiy, S., and Pokrovsky, O.: Microtopography controls of carbon and related elements distribution in the West Siberian frozen bogs, Geosciences, 9, 291, https://doi.org/10.3390/geosciences9070291, 2019.

Lyapina, E. E., Golovatskaya, E. A., and Ippolitov, I. I.: Mercury concentration in natural objects of west Siberia, Contemp. Probl. Ecol., 2, 1–5, https://doi.org/10.1134/S1995425509010019, 2009.

Melendez-Perez, J. J., Fostier, A. H., Carvalho, J. A., Windmöller, C. C., Santos, J. C., and Carpi, A.: Soil and biomass mercury emissions during a prescribed fire in the Amazonian rain forest, Atmos. Environ., 96, 415–422, https://doi.org/10.1016/j.atmosenv.2014.06.032, 2014.

Morel, F. M. M., Kraepiel, A. M. L., and Amyot, M.: The chemical cycle and bioaccumulation of mercury, Annu. Rev. Ecol. Syst., 29, 543–566, https://doi.org/10.1146/annurev.ecolsys.29.1.543, 1998.

Morgalev, Y. N., Lushchaeva, I. V., Morgaleva, T. G., Kolesnichenko, L. G., Loiko, S. V., Krickov, I. V., Lim, A., Raudina, T. V., Volkova, I. I., Shirokova, L. S., Morgalev, S. Y., Vorobyev, S. N., Kirpotin, S. N., and Pokrovsky, O. S.: Bacteria primarily metabolize at the active layer/permafrost border in the peat core from a permafrost region in western Siberia, Polar Biol., 40, 1645–1659, https://doi.org/10.1007/s00300-017-2088-1, 2017.

Obrist, D., Agnan, Y., Jiskra, M., Olson, C. L., Colegrove, D. P., Hueber, J., Moore, C. W., Sonke, J. E., and Helmig, D.: Tundra uptake of atmospheric elemental mercury drives Arctic mercury pollution, Nature, 547, 201–204, https://doi.org/10.1038/nature22997, 2017.

Olson, C., Jiskra, M., Biester, H., Chow, J., and Obrist, D.: Mercury in Active-Layer Tundra Soils of Alaska: Concentrations, Pools, Origins, and Spatial Distribution, Global Biogeochem. Cy., 32, 1058–1073, https://doi.org/10.1029/2017GB005840, 2018.

Osterwalder, S., Sommar, J., Åkerblom, S., Jocher, G., Fritsche, J., Nilsson, M. B., Bishop, K., and Alewell, C.: Comparative study of elemental mercury flux measurement techniques over a Fennoscandian boreal peatland, Atmos. Environ., 172, 16–25, https://doi.org/10.1016/j.atmosenv.2017.10.025, 2018.

Outridge, P. M., Macdonald, E. R. W., Wang, G. F., Stern, G. A., and Dastoor, A. P.: A mass balance inventory of mercury in the Arctic Ocean, Environ. Chem., 5, 89–111, https://doi.org/10.1071/EN08002, 2008.

Panova, N. K., Trofimova, S. S., Antipina, T. G., Zinoviev, E. V., Gilev, A. V., and Erokhin, N. G.: Holocene dynamics of

vegetation and ecological conditions in the southern Yamal Peninsula according to the results of comprehensive analysis of a relict peat bog deposit, Russ. J. Ecol., 41, 20–27, https://doi.org/10.1134/S1067413610010042, 2010.

Pearson, C., Howard, D., Moore, C., and Obrist, D.: Mercury and trace metal wet deposition across five stations in Alaska: controlling factors, spatial patterns, and source regions, Atmos. Chem. Phys., 19, 6913–6929, https://doi.org/10.5194/acp-19-6913-2019, 2019.

Peregon, A., Maksyutov, S., Kosykh, N. P., and Mironycheva-Tokareva, N. P.: Map-based inventory of wetland biomass and net primary production in western Siberia, J. Geophys. Res.-Biogeo., 113, G01007, https://doi.org/10.1029/2007JG000441, 2008.

Peregon, A., Maksyutov, S., and Yamagata, Y.: An image-based inventory of the spatial structure of West Siberian wetlands, Environ. Res. Lett., 4, 045014, https://doi.org/10.1088/1748-9326/4/4/045014, 2009.

Ponomareva, O. E., Gravis, A. G., and Berdnikov, N. M.: Contemporary dynamics of frost mounds and flat peatlands in north taiga of West Siberia (on the example of Nadym site), Earth's Cryosphere, 16, 21–30, 2012 (in Russian).

Preis, Y. and Karpenko, L. V.: Detailed reconstruction of bog functional state as a response to continental climate changes in Holocene (the middle taiga of Western Siberia), Bulletin of the Tomsk Polytechnic University, Geo. Assets Eng., 326, 90–102, 2015 (in Russian).

Prietzel, J., Tyufekchieva, N., Eusterhues, K., Kögel-Knabner, I., Thieme, J., Paterson, D., McNulty, I., de Jonge, M., Eichert, D., and Salomé, M.: Anoxic versus oxic sample pretreatment: Effects on the speciation of sulfur and iron in well-aerated and wetland soils as assessed by X-ray absorption near-edge spectroscopy (XANES), Geoderma, 153, 318–330, https://doi.org/10.1016/j.geoderma.2009.08.015, 2009.

Raudina, T. V., Loiko, S. V., Lim, A. G., Krickov, I. V., Shirokova, L. S., Istigechev, G. I., Kuzmina, D. M., Kulizhsky, S. P., Vorobyev, S. N., and Pokrovsky, O. S.: Dissolved organic carbon and major and trace elements in peat porewater of sporadic, discontinuous, and continuous permafrost zones of western Siberia, Biogeosciences, 14, 3561–3584, https://doi.org/10.5194/bg-14-3561-2017, 2017.

Romanovsky, V. E., Smith, S. L., and Christiansen, H. H.: Permafrost thermal state in the polar Northern Hemisphere during the international polar year 2007–2009: a synthesis, Permafrost Periglac., 21, 106–116, https://doi.org/10.1002/ppp.683, 2010.

Roulet, M., Lucotte, M., Saint-Aubin, A., Tran, S., Rhéault, I., Farella, N., De Jesus Da Silva, E., Dezencourt, J., Sousa Passos, C. J., Santos Soares, G., Guimarães, J. R. D., Mergler, D., and Amorim, M.: The geochemistry of mercury in central Amazonian soils developed on the Alter-do-Chao formation of the lower Tapajos River Valley, Para state, Brazil, Sci. Total Environ., 223, 1–24, https://doi.org/10.1016/S0048-9697(98)00265-4, 1998.

Roulet, M., Lucotte, M., Canuel, R., Farella, N., Courcelles, M., Guimarães, J. R. D., Mergler, D., and Amorim, M.: Increase in mercury contamination recorded in lacustrine sediments following deforestation in the central Amazon, Chem. Geol., 165, 243–266, https://doi.org/10.1016/S0009-2541(99)00172-2, 2000.

Rudmin, M., Ruban, A., Savichev, O., Mazurov, A., Dauletova, A., and Savinova, O.: Authigenic and detrital minerals in peat environment of Vasyugan swamp, western Siberia, Minerals, 8, 500, https://doi.org/10.3390/min8110500, 2018.

Rydberg, J., Klaminder, J., Rosén, P., and Bindler, R.: Climate driven release of carbon and mercury from permafrost mires increases mercury loading to sub-arctic lakes, Sci. Total Environ., 408, 4778–4783, https://doi.org/10.1016/j.scitotenv.2010.06.056, 2010.

Schuster, P. F., Schaefer, K. M., Aiken, G. R., Antweiler, R. C., Dewild, J. F., Gryziec, J. D., Gusmeroli, A., Hugelius, G., Jafarov, E., Krabbenhoft, D. P., Liu, L., Herman-Mercer, N., Mu, C., Roth, D. A., Schaefer, T., Striegl, R. G., Wickland, K. P., and Zhang, T.: Permafrost stores a globally significant amount of mercury, Geophys. Res. Lett., 45, 1463–1471, https://doi.org/10.1002/2017GL075571, 2018 (data available at: https://agupubs.onlinelibrary.wiley.com/action/downloadSupplement?doi=10.1002/2017GL075571&file=grl56886-sup-0002-2017GL075571-ds01.csv and https://agupubs.onlinelibrary.wiley.com/action/downloadSupplement?doi=10.1002/2017GL075571&file=grl56886-sup-0003-2017GL075571-ds02.csv, last access: 15 June 2020).

Selin, N. E., Jacob, D. J., Yantosca, R. M., Strode, S., Jaeglé, L., and Sunderland, E. M.: Global 3-D land-ocean-atmosphere model for mercury: Present-day versus preindustrial cycles and anthropogenic enrichment factors for deposition, Global Biogeochem. Cy., 22, GB2011, https://doi.org/10.1029/2007GB003040, 2008.

Sheng, Y., Smith, L. C., MacDonald, G. M., Kremenetski, K. V., Frey, K. E., Velichko, A. A., Lee, M., Beilman, D. W., and Dubinin, P.: A high-resolution GIS-based inventory of the west Siberian peat carbon pool, Global Biogeochem. Cy., 18, GB3004, https://doi.org/10.1029/2003GB002190, 2004.

Shevchenko, V. P., Pokrovsky, O. S., Vorobyev, S. N., Krickov, I. V., Manasypov, R. M., Politova, N. V., Kopysov, S. G., Dara, O. M., Auda, Y., Shirokova, L. S., Kolesnichenko, L. G., Zemtsov, V. A., and Kirpotin, S. N.: Impact of snow deposition on major and trace element concentrations and elementary fluxes in surface waters of the Western Siberian Lowland across a 1700 km latitudinal gradient, Hydrol. Earth Syst. Sci., 21, 5725–5746, https://doi.org/10.5194/hess-21-5725-2017, 2017.

Skyllberg, U., Qian, J., Frech, W., Xia, K., and Bleam, W. F.: Distribution of mercury, methyl mercury and organic sulphur species in soil, soil solution and stream of a boreal forest catchment, Biogeochemistry, 64, 53–76, https://doi.org/10.1023/A:1024904502633, 2003.

Smieja-Król, B., Fiałkiewicz-Kozieł, B., Sikorski, J., and Palowski, B.: Heavy metal behaviour in peat – A mineralogical perspective, Sci. Total Environ., 408, 5924–5931, https://doi.org/10.1016/j.scitotenv.2010.08.032, 2010.

Smith-Downey, N. V, Sunderland, E. M., and Jacob, D. J.: Anthropogenic impacts on global storage and emissions of mercury from terrestrial soils: Insights from a new global model, J. Geophys. Res., 115, G03008, https://doi.org/10.1029/2009JG001124, 2010.

Soerensen, A. L., Jacob, D. J., Schartup, A. T., Fisher, J. A., Lehnherr, I., St Louis, V. L., Heimbürger, L. E., Sonke, J. E., Krabbenhoft, D. P., and Sunderland, E. M.: A mass budget for mercury and methylmercury in the Arctic Ocean, Global Biogeochem. Cy., 30, 560–575, https://doi.org/10.1002/2015GB005280, 2016.

Sonke, J. E., Teisserenc, R., Heimbürger-Boavida, L. E., Petrova, M. V., Marusczak, N., Le Dantec, T., Chupakov, A. V., Li, C., Thackray, C. P., Sunderland, E. M., Tananaev, N., and Pokrovsky, O. S.: Eurasian river spring flood observations support net Arctic Ocean mercury export to the atmosphere and Atlantic Ocean, P. Natl. Acad. Sci. USA, 115, E11586–E11594, https://doi.org/10.1073/pnas.1811957115, 2018.

St. Pierre, K. A., St. Louis, V. L., Lehnherr, I., Gardner, A. S., Serbu, J. A., Mortimer, C. A., Muir, D. C. G., Wiklund, J. A., Lemire, D., Szostek, L., and Talbot, C.: Drivers of mercury cycling in the rapidly changing glacierized watershed of the High Arctic's largest lake by volume (Lake Hazen, Nunavut, Canada), Environ. Sci. Technol., 53, 1175–1185, https://doi.org/10.1021/acs.est.8b05926, 2019.

Steffen, A., Douglas, T., Amyot, M., Ariya, P., Aspmo, K., Berg, T., Bottenheim, J., Brooks, S., Cobbett, F., Dastoor, A., Dommergue, A., Ebinghaus, R., Ferrari, C., Gardfeldt, K., Goodsite, M. E., Lean, D., Poulain, A. J., Scherz, C., Skov, H., Sommar, J., and Temme, C.: A synthesis of atmospheric mercury depletion event chemistry in the atmosphere and snow, Atmos. Chem. Phys., 8, 1445–1482, https://doi.org/10.5194/acp-8-1445-2008, 2008.

Steinmann, P. and Shotyk, W.: Chemical composition, pH, and redox state of sulfur and iron in complete vertical porewater profiles from two Sphagnum peat bogs, Jura Mountains, Switzerland, Geochim. Cosmochim. Ac., 61, 1143–1163, https://doi.org/10.1016/S0016-7037(96)00401-2, 1997.

Stepanova, V. A., Pokrovsky, O. S., Viers, J., Mironycheva-Tokareva, N. P., Kosykh, N. P., and Vishnyakova, E. K.: Elemental composition of peat profiles in western Siberia: Effect of the micro-landscape, latitude position and permafrost coverage, Appl. Geochem., 53, 53–70, https://doi.org/10.1016/j.apgeochem.2014.12.004, 2015.

Stern, G. A., Macdonald, R. W., Outridge, P. M., Wilson, S., Chételat, J., Cole, A., Hintelmann, H., Loseto, L. L., Steffen, A., Wang, F., and Zdanowicz, C.: How does climate change influence arctic mercury?, Sci. Total Environ., 414, 22–42, https://doi.org/10.1016/j.scitotenv.2011.10.039, 2012.

Talbot, J., Moore, T. R., Wang, M., Ouellet Dallaire, C., and Riley, J. L.: Distribution of lead and mercury in Ontario peatlands, Environ. Pollut., 231, 890–898, https://doi.org/10.1016/j.envpol.2017.08.095, 2017.

Tarnocai, C., Canadell, J. G., Schuur, E. A. G., Kuhry, P., Mazhitova, G., and Zimov, S.: Soil organic carbon pools in the northern circumpolar permafrost region, Global Biogeochem. Cy., 23, 1–11, https://doi.org/10.1029/2008GB003327, 2009.

Trofimova, I. E. and Balybina, A. S.: Classification of climates and climatic regionalization of the West-Siberian plain, Geogr. Nat. Resour., 35, 114–122, https://doi.org/10.1134/S1875372814020024, 2014.

Vasilevich, R. S.: Major and Trace Element Compositions of Hummocky Frozen Peatlands in the Forest–Tundra of Northeastern European Russia, Geochem. Int., 56, 1276–1288, https://doi.org/10.1134/S0016702918100129, 2018.

Velichko, A. A., Timireva, S. N., Kremenetski, K. V., MacDonald, G. M., and Smith, L. C.: West Siberian Plain as a late glacial desert, Quaternary Int., 237, 45–53, https://doi.org/10.1016/j.quaint.2011.01.013, 2011.

Vishnyakova, E. K. and Mironycheva-Tokareva, N. P.: Moss decomposition in Western Siberian mires, in: Mosses: Ecology, Life Cycle and Significance, edited by: Pokrovsky, O., Volkova, I., Kosykh, N., and Shevchenko, V., 4th Edn., Nova Science Publishers Inc., New York, 217–241, 2018.

Wang, X., Yuan, W., Lin, C.-J., Zhang, L., Zhang, H., and Feng, X.: Climate and vegetation as primary drivers for global mercury storage in surface soil, Environ. Sci. Technol., 53, 10665–10675, https://doi.org/10.1021/acs.est.9b02386, 2019.

Wilhelm, R. C., Niederberger, T. D., Greer, C., and Whyte, L. G.: Microbial diversity of active layer and permafrost in an acidic wetland from the Canadian high arctic, Can. J. Microbiol., 57, 303–315, https://doi.org/10.1139/w11-004, 2011.

Zhang, Y., Jacob, D. J., Dutkiewicz, S., Amos, H. M., Long, M. S., and Sunderland, E. M.: Biogeochemical drivers of the fate of riverine mercury discharged to the global and Arctic oceans, Global Biogeochem. Cy., 29, 854–864, https://doi.org/10.1002/2015GB005124, 2015.

Zolkos, S., Krabbenhoft, D. P., Suslova, A., Tank, S. E., McClelland, J. W., Spencer, R. G. M., Shiklomanov, A., Zhulidov, A. V., Gurtovaya, T., Zimov, N., Zimov, S., Mutter, E. A., Kutny, L., Amos, E., and Holmes, R. M.: Mercury export from Arctic great rivers, Environ. Sci. Technol., 54, 4140–4148, https://doi.org/10.1021/acs.est.9b07145, 2020.